COMMISSIONS 27 AND 42 OF THE IAU
INFORMATION BULLETIN ON VARIABLE STARS
Number 6168

Konkoly Observatory
Budapest
25 May 2016

HU ISSN 0374 – 0676

BG CMi TIME KEEPING

BONNARDEAU, MICHEL

MBCAA Observatory, Le Pavillon, 38930 Lalley, France, email: arzelier1@free.fr

BG Canis Minoris (RA=$07^{\rm h}31^{\rm m}29\overset{\rm s}{.}00$, DEC=$+09°56'23\overset{''}{.}1$, J2000) is an intermediate polar (a cataclysmic system in which the white dwarf is magnetized enough to moderate the accretion). Its magnitude is around 14.5. The orbital motion has a period of $P_{\rm orb}$ = 3.235 hr, and gives a modulation visible by photometry.

There is also a modulation of the light curves with a period $P_{\rm spin}$ = 913 s. This modulation is usually interpreted as being due to the spin of the white dwarf. However this is not firmly established: the spin period may be twice $P_{\rm spin}$, with both poles visible (Patterson & Thomas, 1993), or the observed modulation may be synodic, with the spin period being actually shorter (Norton et al., 1992).

According to Pych et al. (1996) and references therein, the period $P_{\rm spin}$ is decreasing, so there is a spin-up of the white dwarf. However, according to Kim et al. (2005, hereafter K05), the rate of this spin-up is decreasing.

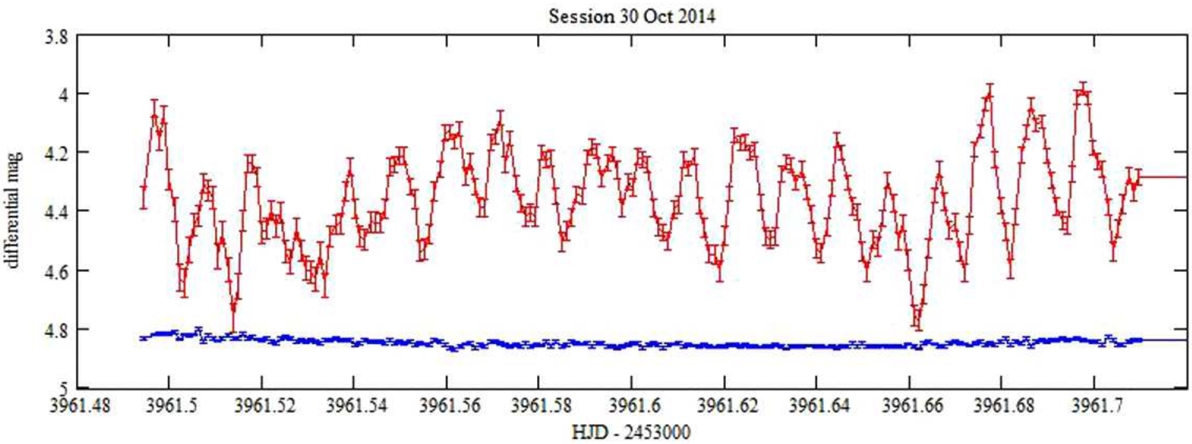

Figure 1. Upper light curve: BG CMi, lower one: the check star shifted by +4.2 mag. The error bars are the quadratic sum of the 1σ statistical uncertainties on the variable/check star and on the comparison star.

Observations

Photometric observations of BG CMi were carried out over twelve seasons, from 2005 to 2016, with a 203 mm f/6.3 Schmidt-Cassegrain telescope, a clear filter and an SBIG ST7E camera (KAF401E CCD). The exposures were 60 s long. For the aperture differential photometry, the comparison star is GSC 768-01373. Over 49 nights 5161 useful images were obtained. A check star, GSC 768-01665, is used to compare the standard deviations to the statistical uncertainties so as to make sure that the systematic errors are low. An example of the light curve is given in Fig. 1.

O-C analysis of the $P_{\rm spin}$ modulation

The light curves are searched for pulses due to the $P_{\rm spin}$ modulation. $N = 254$ well defined pulses are found. These pulses are then fitted with the

$$t(E) = T + PE + BE^2 \tag{1}$$

quadratic ephemeris, where E is the cycle number, minimizing S:

$$S = \sqrt{\frac{\sum_{i=0}^{N-1} (t_i - T - PE_i - BE_i^2)^2/\delta t_i}{\sum_{i=0}^{N-1} 1/\delta t_i}} \tag{2}$$

where the t_i are the HJD of the pulses and the δt_i their uncertainties.

Solution(s) are searched for using a Monte Carlo algorithm. This has the advantage over the least squares method of readily revealing cycle counting ambiguities. It works the following way:

make 10 runs (or more) of the following:

- make 1 millions trials (or more) of the following:
  - select randomly a set of T, P, B;
  - compute the cycle number E_i of each pulse;
  - compute S;
- retain the set of T, P, B that gives the smallest S.

The sets of T, P, B are randomly selected in the following ranges:

- T = [the first pulse$-P_{\rm spin}/2$: the first pulse$+P_{\rm spin}/2$]
- $P = [P_{\rm spin} - P_{\rm spin}/1000 : P_{\rm spin} + P_{\rm spin}/1000]$
- $B = [-40 \times 10^{-13} : 0]$

For each run, the same number of cycles is always obtained, 375,969, between the first and the last pulses. So there is no cycle ambiguity. The adopted values for T, P, B are the average values of the runs, and the adopted values for the uncertainties are the standard deviations:

$$T = 2453449.38837(48)\,\mathrm{HJD} = 2453449.389105\,\mathrm{HJD_{TDB}} \tag{3}$$

$$P = 0.0105726046(47)\,\mathrm{d} \tag{4}$$

$$B = -1.41(11) \times 10^{-13}\,\mathrm{d}. \tag{5}$$

The white dwarf is then spinning up with $\dot{P} = 2B/P = -2.67 \times 10^{-11}$ in a time scale $P/2|\dot{P}| = 543$ kyr.

The ephemeris (1) is precise enough to be applied with no cycle ambiguity to the 2002-2005 data of K05. The cycle numbers run from −76,998 to −4,194.

The spin-up rate in the ephemeris (1) is quite smaller than the one obtained from 1982-1996 observations (Pych et al., 1996),

$$t(e) = T_{\rm P96} + P_{\rm P96}e + B_{\rm P96}e^2, \tag{6}$$

with

$$T_{\rm P96} = 2445020.2800(2)\,\mathrm{HJD} = 2445020.2806\,\mathrm{HJD_{TDB}} \tag{7}$$
$$P_{\rm P96} = 0.010572992(2)\,\mathrm{d} \tag{8}$$
$$B_{\rm P96} = -3.83(4) \times 10^{-13}\,\mathrm{d}. \tag{9}$$

When the ephemeris (6) is applied to the 2002-2005 data of K05, the first pulse is at the epoch number $-720,254$, with an ambiguity of ± 1 or more cycles.

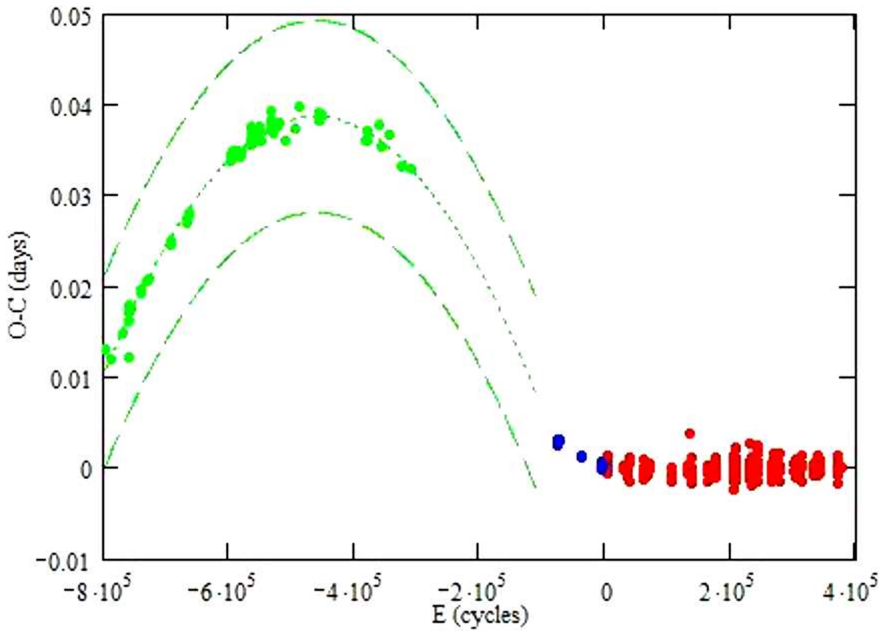

Figure 2. Red dots: present data, Blue: K05, Green: Pych et al (1996) with the first pulse between the epochs $-720,254$ and $-76,998$. Green dotted line: ephemeris (2) with $E = e + E_0$, upper dashed line: with $E = e + E_0 + 1$, lower dashed line: with $E = e + E_0 - 1$.

Besides the heliocentric correction, there are smaller corrections to be taken into account (Eastman et al., 2010), in particular the leap seconds due to the Earth rotation slowing down. The leap second correction at the time of the ephemeris (1), in 2005, is 32 s, and 36 s in 2016. And at the time of ephemeris (2), in 1982, it is 20 s, and 30 s in 1996. The barycentric effect of Jupiter and Saturn is neglected as it is only ± 4 s and cyclic (unlike the leap seconds that keep accumulating), and the other general relativistic corrections are much smaller. (And there is also 32.184 s to be added to obtain BJD_{TDB}.)

This gives the O−C diagram in Fig. 2, computed from the ephemeris (1).

Between 1996 and 2005 there was a change of regime, from the ephemeris (6) to the ephemeris (1). Unfortunately, this was not observed, except by K05 who captured the end of this episode.

Fourier analysis of the orbital modulation

The light curves are inspected to look for the orbital dips, and they are found in phase with the orbital ephemeris of K05.

The light curves are analysed with the Period04 software program (Lenz & Breger, 2005), which provides simultaneously sine-wave fitting and least-squares fitting algorithms, around the frequency $1/P_{\rm orb}$. Besides $1/P_{\rm orb}$, up to 6 harmonics are used to fit the orbital modulation. This yields the orbital period:

$$P_{\rm orb} = 0.134748376(74)\,{\rm d} \tag{10}$$

which is in agreement with the period of K05 (the uncertainty is given by the Period04 Monte Carlo simulation).

Fourier analysis of the residuals

As the $P_{\rm spin}$ period is varying, the data are analysed season by season (so the variation is not too important): for each season an average $P_{\rm spin}$ period is computed from the ephemeris (1) and the Period04 program is used to derived the amplitude and phase. The same is done for 2 harmonics (actually, the amplitudes of these 2 harmonics are very small: the modulation is quasi-sinusoidal).

The data are then prewhitened with this fit for the $P_{\rm spin}$ modulation and with the fit for the orbital modulation, yielding a Fourier spectrum of the residuals for the season.

These Fourier spectra show many variations from one season to the other. But it is not clear which have physical causes. Actually, such features were already observed (Patterson & Thomas, 1993, Garlick et al., 1994, de Martino et al., 1995). All these spectra for each season are summed, resulting in a spectrum for the whole set of observations, prewhitened with the $P_{\rm spin}$ and the orbital modulations. Most of the variations cancel out, and a fairly strong peak shows up with two fainter ones, as shown in Figure 3.

The peak (1) corresponds to a period of 1083 s. It was already observed by Patterson & Thomas (1993) who interpreted it as the sideband $1/P_{\rm spin} - 2/P_{\rm orb}$.

The peak (2) corresponds to a period of 1309 s. It has not been reported by other observers. It could be the sideband $1/P_{\rm spin} - 4/P_{\rm orb}$.

The peak (3) corresponds to a period of 835 s. This is close to the signal at 847 s reported by Norton et al. (1992) and Choi et al. (2007) in X-ray, but unseen in optical band except by Garlick et al. (1994), and which was interpreted as the sideband $1/P_{\rm spin}+1/P_{\rm orb}$.

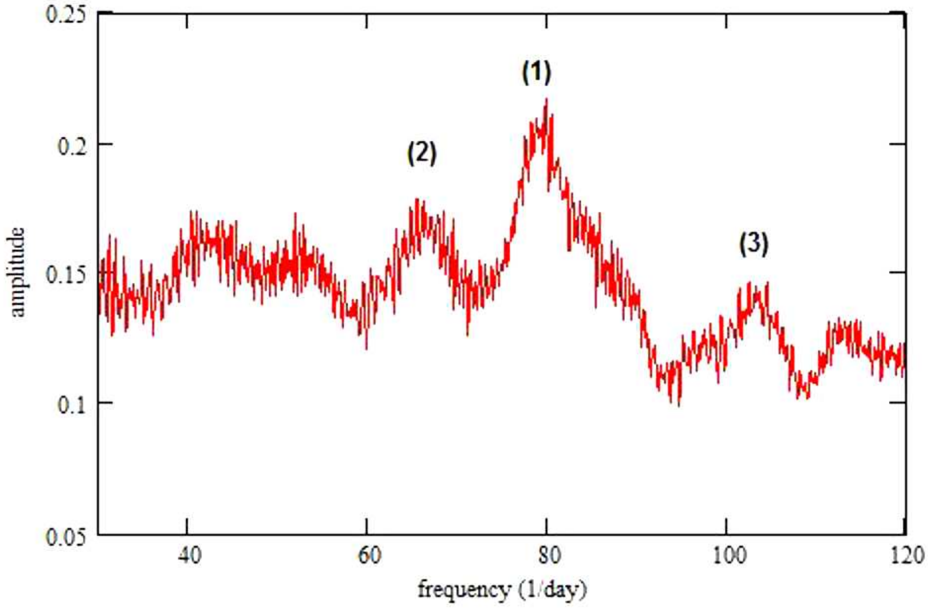

Figure 3. Sum of the spectra of the residuals for the twelve seasons.

References:

Choi C.-S., Dotani T., Kim Y., Ryu D., 2007, *New Astronomy*, **12**, 622
de Martino D. et al., 1995, *A&A*, **298**, 849
Eastman J., Siverd R., Gaudi B.S., 2010, *PASP*, **122**, 935
Garlick M.A. et al., 1994, *MNRAS*, **267**, 1095
Kim Y.G., Andronov I.L., Park S.S., Jeon Y.B., 2005, *A&A*, **441**, 663
Lenz P., Breger M., 2005, *Comm. Asteroseismology*, **146**, 53
Norton A.J., McHardy I.M., Lehto H.J., Watson M.G., 1992, *MNRAS*, **258**, 697
Patterson J., Thomas G., 1993, *PASP*, **105**, 59
Pych W., Semeniuk I., Olech A., Ruszkowski M., 1996, *Acta Astronomica*, **46**, 279